In-situ interface self-assemblies of nanocrystalline Ag₂E (E=S, Se, or Te) *via* chalcogen directional transfer agents

Xuchuan Jiang, Yi Xie,* Jun Lu, Liying Zhu, Wei He and Yitai Qian

Structure Research Laboratory and Laboratory of Nanochemistry & Nanomaterials, University of Science & Technology of China, Hefei, Anhui, 230026, P. R. China. E-mail: yxie@ustc.edu.cn

Nanocrystalline Ag₂E (E=S, Se, or Te) was interface self-assembled *in-situ* in the heterogeneous microphase *via* the reaction of aqueous AgNO₃ and R=E (R=PPh₃, PBu₃, PCy₃ or Py; E=S, Se, or Te) toluene solution at room temperature. Chalcogen directional transfer agents R=E were prepared by refluxing in toluene solution for 12 h. The compositions of as-prepared products were characterized by X-ray powder diffraction (XRD) and X-ray photoelectron spectroscopy (XPS). The atomic ratios of Ag to S, Se or Te, measured by inductively coupled plasma (ICP) spectroscopy, were 1.98 : 1, 2.08 : 1 and 2.13 : 1, respectively. The morphologies of products were confirmed by transmission electron microscopy (TEM). UV-Visible spectroscopy was used to record the absorption of Ag₂E nanocrystallites after removal of the passivated molecules at high temperature (>500 °C). The thermal stability of Ag₂E particles passivated by R=E (R=PPh₃, PBu₃, PCy₃ or Py) molecules was studied using thermal gravimetric analysis (TGA). The possible mechanism of nanocrystalline silver chalcogenide self-assembly is discussed.

Introduction

Late transition metal chalcogenides have a number of commercial applications in pigments, semiconductors and fluorescence devices.[1] Silver chalcogenide nanometric semiconductors have good optoelectronic and thermoelectric properties. Silver sulfide nanometric semiconductors, as well as other silver chalcogenides, are good prospective optoelectronic and thermoelectric materials often used as photosensitizers for photographic purposes.[2] Silver selenide, a well-known superionic conductor,[3] has been used to prepare nonlinear optical devices,[4] photochargeable secondary batteries,[5] and multipurpose ion-selective electrodes.[6]

For the above-mentioned applications, a wide range of techniques have been developed to prepare silver chalcogenides with controlled microstructure and particle size. Bulk silver sulfide could be prepared *via* the combination of two kinds of elements or the precipitation from a solution of Ag⁺ ions with S²⁻ ions. The thin film of Ag₂S semiconductor deposited in solution was studied by several researchers.[7] The silver chalcogenide nanoparticles prepared *via* wet chemical methods such as reverse micelles,[8] decomposed precursor molecules method,[9] liquid crystal templates,[10] and the CS₂ reduction method have been widely investigated.[11] Moreover, mechanical alloying ball mill,[12] electrolysis,[13] and hydrothermal[14] methods have also been used to synthesize silver chalcogenides. Recently, Parkin and co-workers reported the synthesis of silver chalcogenides by elemental reaction *via* amine-assisted routes such as *n*-hexylamine, 1,2-diaminoethane, aqueous ammonia solution and liquid amines.[15]

In this work, we designed a novel route for the assembly of silver chalcogenide nanocrystallites *via* the reaction of Ag⁺ ions with S, Se or Te directional transfer agents such as PPh₃, PBu₃, PCy₃ or Py in the heterogeneous microphase formed at a two-phase interface under ambient conditions. The compositions and properties of silver chalcogenides were characterized and investigated by XRD, XPS, TEM, UV-visible and TGA techniques. The possible self-assembly mechanism of chalcogen directional transfer agents with

Ag⁺ ions was discussed. This novel method could be extended to the synthesis of more transition metal chalcogenides.

Experimental

Reagents

The reagents used, including triphenylphosphine (PPh₃), tributylphosphine (PBu₃), tricyclohexylphosphine (PCy₃), pyridine (Py), toluene, powders of elemental sulfur, selenium and tellurium, and silver nitrate were all of analytical grade. Distilled water was used throughout.

Procedure

The procedure for synthesizing Ag₂E (E=S, Se or Te) nanocrystallites was as follows. First, preparation of chalcogen directional transfer agents R=E (R=PPh₃, PBu₃, PCy₃ or Py). The same general reaction scale and procedure as described here for Ph₃P=E was adopted for all the reactions. Briefly, 0.002 mol Ph₃P and 0.001 mol sulfur, selenium or tellurium powders were added into a 200 ml three-neck flask with 100 ml toluene and refluxed for 12 h. The Ph₃P=E complex formed according to the literature.[16] After cooling to room temperature, the mixture was filtered and the residue stored. Secondly, *in-situ* interface self-assemblies of Ag₂E were prepared by slowly adding a 60 ml Ph₃P=E toluene solution (0.002 mol [0.524 g] Ph₃P in 100 ml toluene) into a 150 ml beaker containing 60 ml 0.02 mol dm⁻³ aqueous AgNO₃ solution. The beaker was then left in the dark for 72 h. Black products formed at the interface between the toluene and aqueous phases which were centrifuged, filtered, and washed with distilled water and ethanol, respectively, then dried in a vacuum at 40 °C for 2 h.

Characterization

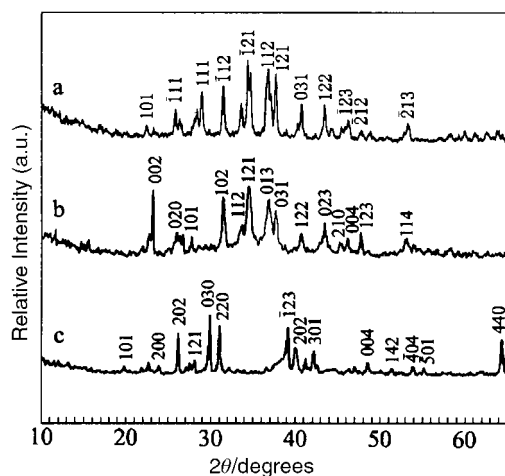The three samples were characterized as follows. The XRD analysis was carried out with a Japan Rigaku D/max-γ

Fig. 1 The XRD patterns for Ag$_2$S (a), Ag$_2$Se (b) and Ag$_2$Te (c) nanocrystallites.

rotation anode X-ray diffractometer, using Ni-filtered Cu-Kα radiation ($\lambda = 1.54178$ Å). A scanning rate of $0.05°\,s^{-1}$ was applied to record the patterns in the 2θ range of 10–65°. The reflection data were collected at 25 °C. The electronic binding energy of silver chalcogenides was examined by X-ray photoelectron spectroscopy (XPS) on an ESCALab MKII instrument with Mg-Kα ($h\nu = 1253.6$ eV) radiation as the excitation source with an energy resolution of 1.0 eV. TEM images were taken with a Hitachi H-800 transmission electron microscope at an acceleration voltage of 200 kV. The Ag$_2$E powders were ultrasonically redispersed in ethanol, and one drop of solution was adsorbed onto the copper grid for measurement. The atomic ratios of silver chalcogenides were measured using inductively coupled plasma (ICP) spectroscopy with a Seiko Electronics SPD 1200A ICP emission analyzer with a pump flow of $1.85\,\text{ml min}^{-1}$ and the flow rate of auxiliary gas (Ar 99.99%) $0.5\,\text{l min}^{-1}$. The samples were dissolved in a heated dilute HNO$_3$ solution and further elemental analysis was carried out according to the literature.[17] Elemental Se and Te are similar to S in some aspects of their chemical properties, thus, the atomic ratios of Ag$_2$Se and Ag$_2$Te were also analyzed according to the literature[17] in our experiments. UV-Vis absorption spectra were recorded using a UV-visible Spectrophotometer Specord 200 in the 190–1100 nm wavelength range (Analytik Jena GmbH, Germany). The thermal stability of Ag$_2$E particles adsorbed by R=E molecules was measured by thermal gravimetric analysis (Shimadzu TGA-50H, Japan) with a flow rate of $20.0\,\text{ml min}^{-1}$ and a heating rate of $10\,°\text{C min}^{-1}$. Hydrodynamic measurements of microphases were taken on a Malvern 2000 light scattering system equipped with a Spectra Physics 171 argon ion laser, a digital correlator, micro-

computer, and refractive index matched optical specimen cell assembly at 25 °C.

Results and discussion

The XRD patterns are shown in Fig. 1 for Ag$_2$S (a), Ag$_2$Se (b), and Ag$_2$Te (c), respectively. The indexed reflection peaks broaden in each XRD pattern of these samples, indicating that polycrystalline Ag$_2$E nanoparticles form. All the reflection peaks in each XRD pattern are used to calculate the cell parameters and particle sizes of Ag$_2$E (Table 1) by means of the Scherrer formula.[18]

Here the silver chalcogenides are obtained *via* the self-assembly reaction of Ag$^+$ ions and chalcogen directional transfer agents at room temperature. The monoclinic symmetry of the Ag$_2$S phase is similar to that obtained from the reaction of AgNO$_3$ and H$_2$S.[19] However, Parkin and co-workers obtained cubic symmetry for Ag$_2$S (JCPDS no. 4-774) by elemental reaction *via* amine-assisted routes at ambient conditions,[15] which is a high temperature (>179 °C) phase.[20] In addition, the Ag$_2$Te obtained here has monoclinic symmetry (JCPDS no. 34-142), which is different from that reported for Ag$_2$Te prepared *via* elemental reaction (monoclinic symmetry, JCPDS no. 42-1266).[15] Only the Ag$_2$Se (orthorhombic symmetry) obtained in our experiments is the same as that reported by Parkin.[15] Moreover, we obtain phase-pure Ag$_2$Te *via* the self-assembly reaction. This difference is possibly due to the different solvents used in these reaction systems.

Fig. 2 shows the XPS spectra of silver chalcogenides. The binding energy values of Ag 3d (a) are 368.1 eV for Ag$_2$S, 367.9 eV for Ag$_2$Se and 367.6 eV for Ag$_2$Te, respectively, which are in good agreement with those reported in the literature.[21] Therefore, we consider that the order of bond strength is Ag–S $>$ Ag–Se $>$ Ag–Te. All the shapes of the Ag 3d peaks in Ag$_2$E are similar. In addition, the kinetic energy values of AgMNN (b) are 356.1 eV for Ag$_2$S, 356.3 eV for Ag$_2$Se and 356.6 eV for Ag$_2$Te, which are also in accord with the literature.[21] The atomic ratios of Ag$_2$E obtained from the integrated areas of the Ag 3d (a) and S 2p (c), Se 3d (d) or Te 3d (e) peaks, are 1.96 : 1, 2.12 : 1 and 2.18 : 1, respectively, which are nearly consistent with those obtained from ICP elemental analysis (Ag$_{1.98}$S, Ag$_{2.08}$Se and Ag$_{2.13}$Te).

The product morphologies are confirmed by the TEM observations shown in Fig. 3. After the mixture of R=E (in toluene) and aqueous AgNO$_3$ solutions had been left for 72 h, the black products formed at the interface of the two phases were centrifuged, washed and redispersed in ethanol for TEM measurement. Square-like Ag$_2$S (a), spherical Ag$_2$Se (b) and Ag$_2$Te (c) nanocrystallites were obtained, and the particle diameters determined from the TM images are *ca.* 43, 19 and 32 nm, respectively. Meanwhile, the electronic diffraction (ED) rings of products are all indexed, indicating that they are polycrystallites, which is consistent with the indexed XRD patterns.

The mechanism of the *in-situ* self-assembly of nanocrystal-

Table 1 The cell parameters and particle sizes (calculated using the Scherrer formula) of Ag$_2$E (E = S, Se or Te)

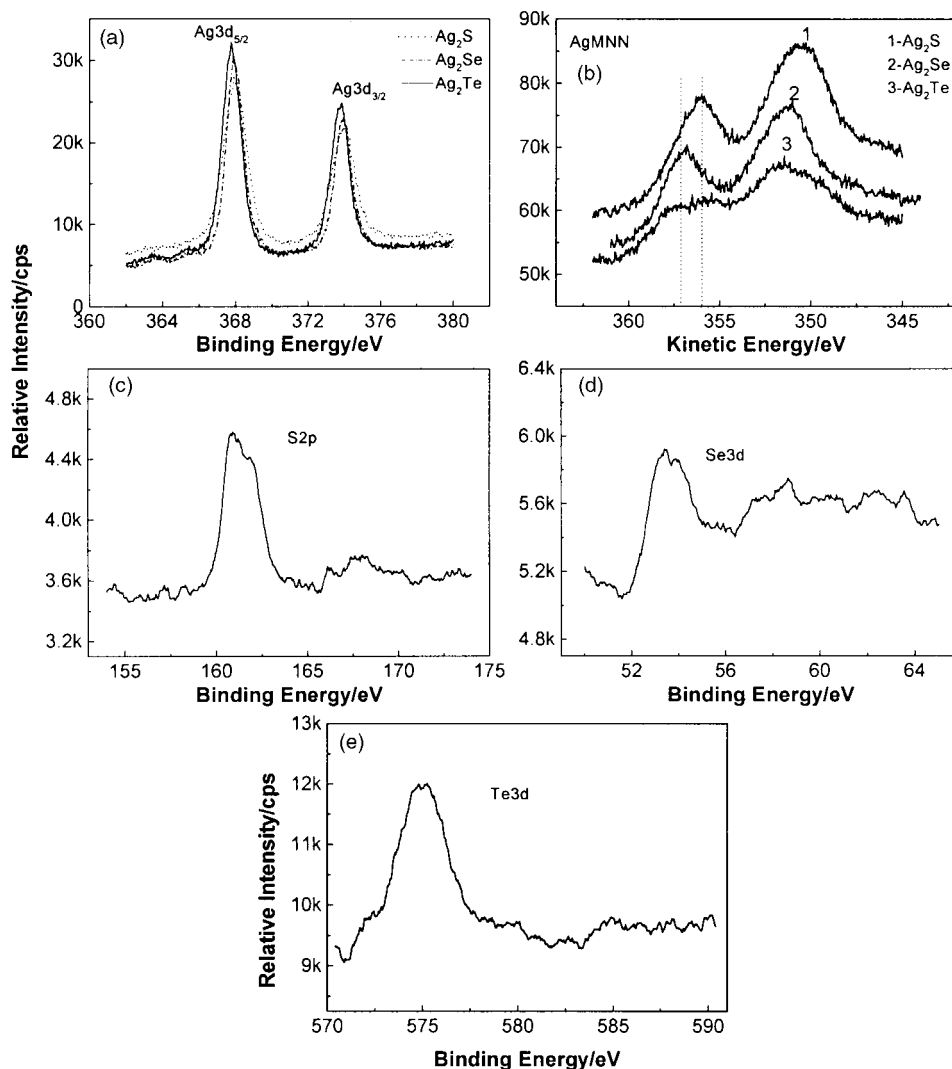| Samples | Cell parameters/Å | | Crystal symmetry | JCPDS | Diameter/nm |
	Calculation	Lit. values			
Ag$_{1.98}$S	$a = 4.182 \pm 0.034$ $b = 6.843 \pm 0.043$ $c = 7.770 \pm 0.052$	$a = 4.229$ $b = 6.931$ $c = 7.862$	Monoclinic	14-72	$\sim$40
Ag$_{2.08}$Se	$a = 4.302 \pm 0.048$ $b = 6.905 \pm 0.095$ $c = 7.672 \pm 0.073$	$a = 4.333$ $b = 7.062$ $c = 7.764$	Orthorhombic	24-1041	$\sim$21
Ag$_{2.13}$Te	$a = 8.038 \pm 0.056$ $b = 8.839 \pm 0.036$ $c = 8.010 \pm 0.045$	$a = 8.169$ $b = 8.940$ $c = 8.065$	Monoclinic	34-142	$\sim$29

Fig. 2 XPS spectra of Ag_2E (E = S, Se or Te): (a) Ag 3d spectra, (b) AgMNN spectra, (c) S 2p, (d) Se 3d, and (e) Te 3d spectra.

line Ag_2E is proposed. The hydrodynamic measurements of the microphase show that no reverse micelles form at the interface.[22] Scheme 1 illustrates the self-assembly processes of chalcogen directional transfer agents reacting with Ag^+ ions in the heterogeneous microphase. The R=E molecules are disordered in toluene solution, whilst they are ordered at the interface of the two phases due to the tendency of R=E to react with Ag^+ ions and their hydrophobic R groups. Fendler and co-workers reported the epitaxial growth of PbS,[23] $PbSe$,[24] and CdS[25] semiconductor nanocrystallites under arachidic acid
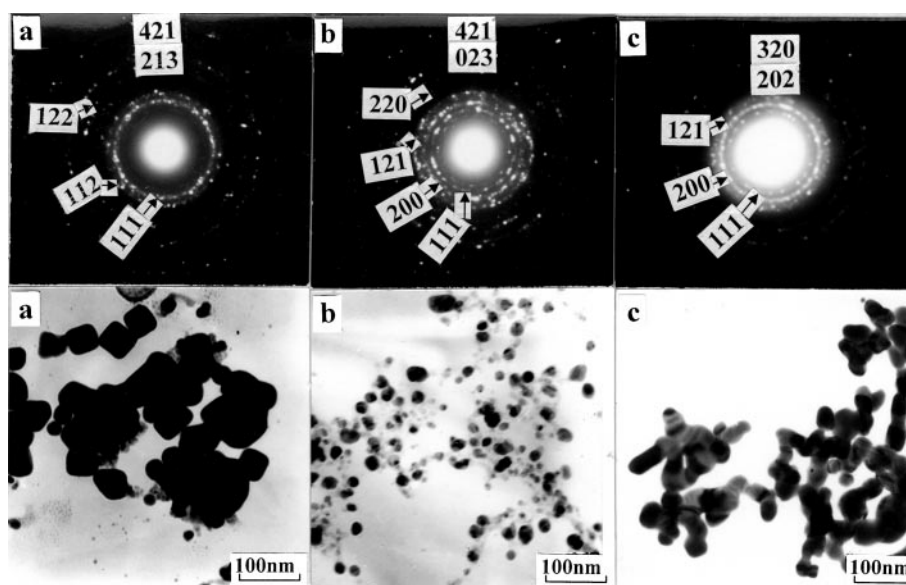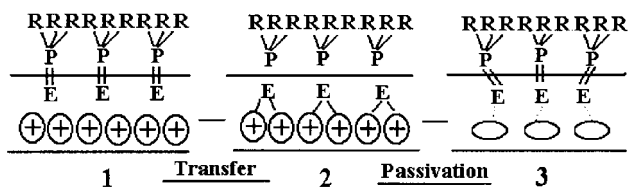

Fig. 3 TEM images and ED patterns of products: (a) square-like Ag_2S, (b) spherical Ag_2Se, and (c) spherical Ag_2Te.

Scheme 1 Illustration of the self-assembly processes of chalcogen directional transfer agents with Ag$^+$ ions. Here R = Ph, Bu, Cy or Py; E = S, Se or Te.

$[CH_3(CH_2)_{18}CO_2H]$ monolayers, suspended in aqueous lead nitrate solution, which is a microphase formed by surfactant self-assembly at the two-phase interface. Here the tendency of Ag$^+$ ions reacting with E atoms makes the R=E molecules order at the interface in a similar manner to surfactants.[23–25] Once the aqueous AgNO$_3$ and the Ph$_3$P=E toluene solutions contact, a heterogeneous microphase forms at the two-phase interface. The chalcogen transfer reaction occurs due to the weak double bond of the R=E molecules[16] and the greater stability of the Ag$_2$E product. The chalcogen directional transfer agents could self-assemble into supramolecules, utilizing the solubility differences between the organic and aqueous phases, and the tendency of E atoms in R=E molecules to react with Ag$^+$ ions in the heterogeneous microphase. The well-packed supramolecules provide the initial templates as nanoreactors for the nucleation and growth of Ag$_2$E nanocrystallites, which is similar to the growth of CdS under the monolayer on the surface of sub-phases.[25] Each of the Ag$_2$E particles formed attracts additional S, Se or Te in R=E molecules from the organic phase and Ag$^+$ ions from the aqueous phase; in the meantime, the size of the R=E domains increases. The increased R=E domains, in turn, permit further growth of the Ag$_2$E nanoparticles. The process continues as long as a match exists between the S, Se or Te headgroups of the R=E molecules and the Ag$^+$ ions in the heterogeneous microphase. This mechanism is also similar to that reported in the literature.[26] We also found that the reaction rate for reactions of Ag$^+$ ions and R=E is in the order: R=S > R=Se > R=Te. The nucleation of Ag$_2$E nanoparticles may be fast but the 72 h reaction time is required for the crystallization. Moreover, the R=E molecules also act as stabilizers, preventing the products from precipitating from the two-phase interface. The passivation of R=E molecules on the surfaces of Ag$_2$E nanoparticles is similar to that for the TBP (tributylphosphate)[27] or TOPO (tri-*n*-octylphosphine oxide) molecules capped on CdSe nanocrystallites.[28,29]

UV-Visible spectra of products (Fig. 4) were obtained from the supernatants of Ag$_2$E powders redispersed in heptane solution. The absorption bands of Ag$_2$E are broadened and each has a long absorption tail at 700–1100 nm. The absorption maximum of Ag$_2$S is around 604 nm, which is consistent with
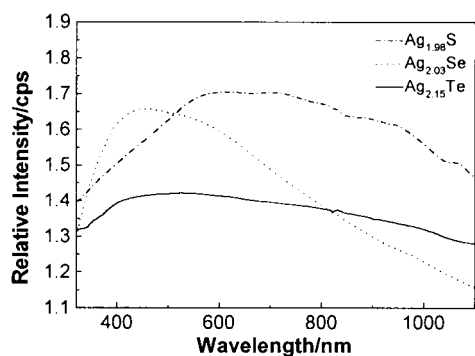

Fig. 4 UV-Visible spectra of Ag$_2$E (E = S, Se or Te) nanoparticles obtained from the supernatants of powders redispersed in heptane solution.
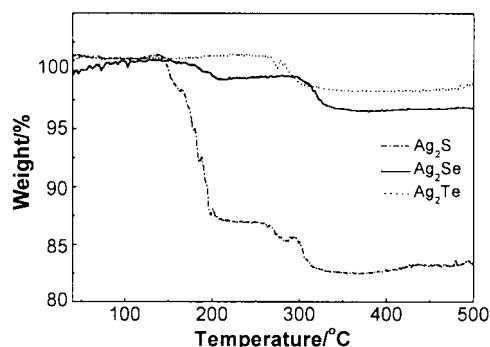

Fig. 5 TGA spectra of PPh$_3$=E (E = S, Se or Te) passivated on the surface of Ag$_2$E (E = S, Se or Te) nanoparticles. The heating rate is 10 °C min^{-1}.

that reported in the literature.[30] The absorption maxima of Ag$_2$Se and Ag$_2$Te are around 462 nm and 522 nm, respectively, in our experiments.

The thermal stability of R=E passivated on the Ag$_2$E nanoparticles was studied using thermal gravimetric analysis (TGA). Fig. 5 shows that the weight losses for Ag$_2$E nanoparticles self-assembled in the heterogeneous microphase at the interface between the Ph$_3$P=E–toluene and aqueous AgNO$_3$ solutions are 16.8 wt% for Ag$_2$S, 3.92 wt% for Ag$_2$Se, and 2.32 wt% for Ag$_2$Te, respectively. The number of molecules passivated on the surface of Ag$_2$E nanoparticles are in the order of Ph$_3$P=S > Ph$_3$P=Se > Ph$_3$P=Te. In addition, the weight loss of Ag$_2$S at 141.9–198.6 °C is considered to be due to the evaporation of some molecules[31] ($\sim$11.2 wt%) and the weight loss at 261.3–305.2 °C ($\sim$5.6 wt%) accounts for the desorption of the remaining Ph$_3$P=S from the surface of the Ag$_2$S nanoparticles. Similarly, the weight loss at 179.1–200.2 °C ($\sim$1.1 wt%) accounts for the evaporation of some of the Ph$_3$P=Se molecules[31] from the surface of Ag$_2$Se with the remainder being lost at 297.9–308.4 °C ($\sim$2.8 wt%). For Ag$_2$Te nanoparticles, by contrast, desorption of Ph$_3$P=Te molecules is only observed at 261.2–309.3 °C. From the weight losses observed, the chemical affinity of Ph$_3$P=E molecules on the surface of Ag$_2$E nanoparticles appears to be in the order Ph$_3$P=S > Ph$_3$P=Se > Ph$_3$P=Te in agreement with the earlier discussion.

This work designed a novel chalcogen directional transfer route to the self-assembly of silver chalcogenide nanocrystallites in the heterogeneous microenvironment of the organic–inorganic phase interface at ambient conditions. This could be widely extended to the assembly of more varied nanometric materials in a heterogeneous microphase.

Acknowledgement

References

1 (*a*) N. N. Greenwood and E. A. Earnshaw, *Chemistry of the Elements*, Pergamon, Oxford, 1990, p. 1403; (*b*) G. Nickless, *Inorganic Chemistry of Sulphur*, Elsevier, London, 1968, p. 670

2 G. L. DeRycke and F. Henderickx, European Patent Application no. 89202613, 9, 1990.

3 (*a*) F. Shimojo and H. Okazaki, *J. Phys. Soc. Jpn.*, 1993, **62**, 179; (*b*) K. Honma and K. Iida, *J. Phys. Soc. Jpn.*, 1987, **56**, 1828; (*c*) T. Sakuma, K. Iida, K. Honma and H. Okazaki, *J. Phys. Soc. Jpn.*, 1977, **43**, 538.

4 K. L. Lewis, A. M. Pitt, T. Wyatt-Davies and J. R. Milward, *Mater. Res. Soc. Symp. Proc.*, 1994, **374**, 105.

5 T. Akoto, Y. Hasuda, M. Ishizawa and T. Horie, *Jpn. Kokai Tokkyo Koho* JP 04. 171, 681 [92, 171, 681].

6 B. Nesie and M. S. Jovanovic, *J. Serb. Chem. Soc.*, 1991, **56**, 353.

7   (a) I. Grozdanov, *Appl. Surf. Sci.*, 1995, **84**, 325; (b) M. Ristova and P. Toshev, *Thin Solid Films*, 1992, **216**, 274.
8   (a) C. Petit, P. Lixon and M. P. Pileni, *J. Phys. Chem.*, 1993, **97**, 12974; (b) L. Motte, F. Billudet and M. P. Pileni, *J. Mater. Sci.*, 1996, **31**, 38.
9   Y. Xie, P. Yan and Y. T. Qian, *Chem. Lett.*, 1999, 655.
10 P. V. Braun, P. Osener, V. Tohver, S. B. Kennedy and S. I. Stupp, *J. Am. Chem. Soc.*, 1999, **121**, 7302.
11 C. Wang, X. Zhang, X. Qian, W. Wang and Y. Qian, *Mater. Res. Bull.*, 1998, **33**, 1083.
12 T. Ohtani, K. Maruyama and K. Ohshima, *Mater. Res. Bull.*, 1997, **32**, 343.
13 A. M. De Becdelievre, J. Amosse and M. J. Barbier, *Mater. Res. Bull.*, 1970, **5**, 367.
14 (a) L. Cambi and M. Elli, *Chim. Ind. (Milan)*, 1968, **50**, 94; (b) W. Wang, Y. Geng, Y. T. Qian, M. R. Ji and Y. Xie, *Mater. Res. Bull.*, 1999, **34**, 877.
15 (a) V. Dusastre, B. Omar, I. P. Parkin and G. Shaw, *J. Chem. Soc., Dalton Trans.*, 1997, 3505; (b) G. Henshaw, I. P. Parkin and G. Shaw, *J. Chem. Soc., Dalton Trans.*, 1997, 231; (c) G. Henshaw, I. P. Parkin and G. Shaw, *Chem. Commun.*, 1996, 1095.
16 K. B. Capps, B. Wixmerten, A. Bauer and C. D. Hoff, *Inorg. Chem.*, 1998, **37**, 2861.
17 J. H. Karchmer, ed., *The Analytical Chemistry of Sulfur and its Compounds*, Part 1, Wiley, New York, 1970.
18 C. N. J. Wagner and E. N. Aqua, *Adv. X-Ray Anal.*, 1964, **7**, 46.
19 *Nat. Bur. Stand. (US) Monogr.*, 1960, **539**, 51.
20 Rahlfs, *Z. Phys. Chem.*, 1935–36, **31**, 157.
21 C. D. Wagner, W. W. Riggs, L. E. Davis, J. F. Moulder and G. E. Muilenberg, *Handbook of X-Ray Photoelectron Spectroscopy*, Perkin-Elmer Corporation, Physical Electronics Division, USA, 1979.
22 K. Kurihara, J. Kizling, P. Stenius and J. H. Fendler, *J. Am. Chem. Soc.*, 1983, **105**, 2574.
23 X. Zhao, L. D. McCormick and J. H. Fendler, *Adv. Mater.*, 1992, **4**, 93.
24 J. Yang, J. H. Fendler, T.-C. Jao and T. Laurion, *Microsc. Res. Tech.*, 1993, **27**, 402.
25 J. Yang, F. C. Meldrum and J. H. Fendler, *J. Phys. Chem.*, 1995, **99**, 5500.
26 J. Yang and J. H. Fendler, *J. Phys. Chem.*, 1995, **99**, 5505.
27 Y. Xie, P. Yan, J. Lu, Y. T. Qian and S. Y. Zhang, *Chem. Commun.*, 1999, 1967.
28 X. G. Peng, J. Wickham and A. P. Alivisatos, *J. Am. Chem. Soc.*, 1998, **120**, 5343.
29 J. K. Lorenz and A. B. Ellis, *J. Am. Chem. Soc.*, 1998, **120**, 10970.
30 L. Motte, F. Billoudet and M. P. Pileni, *J. Phys. Chem.*, 1995, **99**, 16425.
31 J. A. Dean, ed., *Langes Handbook of Chemistry*, 13th edn., R. R. Donnelley & Sons, Inc., USA, 1972, 7-681: t748, t749.